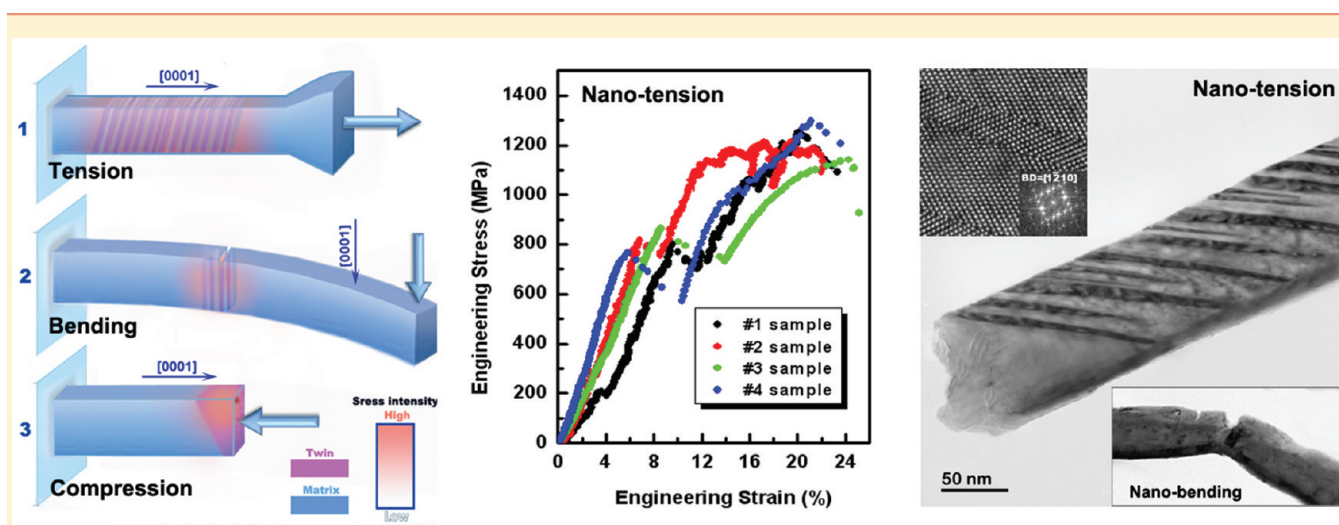


## The Nanostructured Origin of Deformation Twinning

Qian Yu,<sup>†,‡,□</sup> Liang Qi,<sup>§,⊥,□</sup> Kai Chen,<sup>⊥</sup> Raja K. Mishra,<sup>¶</sup> Ju Li,<sup>§,||,⊥</sup> and Andrew M. Minor<sup>\*,†,‡</sup><sup>†</sup>Department of Materials Science and Engineering, University of California, Berkeley, California 94720, United States<sup>‡</sup>National Center for Electron Microscopy, Lawrence Berkeley National Laboratory, Berkeley, California 94720, United States<sup>§</sup>Department of Nuclear Science and Engineering and <sup>||</sup>Department of Materials Science and Engineering, Massachusetts Institute of Technology, Cambridge, Massachusetts 02139, United States<sup>⊥</sup>State Key Laboratory for Mechanical Behavior of Materials and Frontier Institute of Science and Technology, Xi'an Jiaotong University, Xi'an 710049, China<sup>¶</sup>General Motors Research and Development Center, Warren, Michigan 48090, United States

## Supporting Information



**ABSTRACT:** We have revealed the fundamental embryonic structure of deformation twins using in situ mechanical testing of magnesium single crystals in a transmission electron microscope. This structure consists of an array of twin-related laths on the scale of several nanometers. A computational model demonstrates that this structure should be a generic feature at the incipient stage of deformation twinning when there are correlated nucleation events. Our results shed light on the origin of twinning-induced plasticity and transformation toughening, critical to the development of advanced structural alloys with high strength, ductility, and toughness.

**KEYWORDS:** *In situ TEM tensile/bending/compression tests, high-strength Mg, nanotwin, TWIP, nucleation*

Hexagonal close-packed magnesium alloys are only ~30% heavier than some common plastics, and their increased use could greatly impact society in areas such as automotive fuel economy.<sup>1</sup> However, coarse-grained Mg alloys have poor formability and energy-absorbing characteristics due to the absence of five “easy” dislocation slip systems in hexagonal close-packed crystals. In some alloys, energy absorption can be greatly enhanced by deformation twinning, a collective inelastic dissipation mode<sup>2,3</sup> frequently seen in hexagonal close-packed metals.<sup>4–6</sup> There have been many efforts over the years to provide a description for the fundamental nucleation and growth mechanisms of deformation twinning,<sup>7–11</sup> but a consensus has not emerged. Certain deformation twinning modes are thought to be beneficial to the ductility of Mg,<sup>12</sup> while others are considered detrimental.<sup>12,13</sup> In advanced alloys

such as TWIP (twinning-induced plasticity) steels,<sup>14,15</sup> deformation twinning has been engineered to give significantly enhanced ductility and toughness. Since twin boundaries impede dislocation motion,<sup>13,16</sup> twin boundaries generated during deformation harden the material. However, the reorientation of the crystal due to twinning changes the ability of dislocations to move, which can lead to softening.<sup>12,17</sup> Thus, deformation twinning can be used to fine-tune the mechanical properties of an alloy to achieve an optimal value of strength and ductility, and understanding the origin of deformation twinning could open up new avenues for alloy design.

**Received:** November 10, 2011

**Revised:** December 22, 2011

**Published:** January 12, 2012

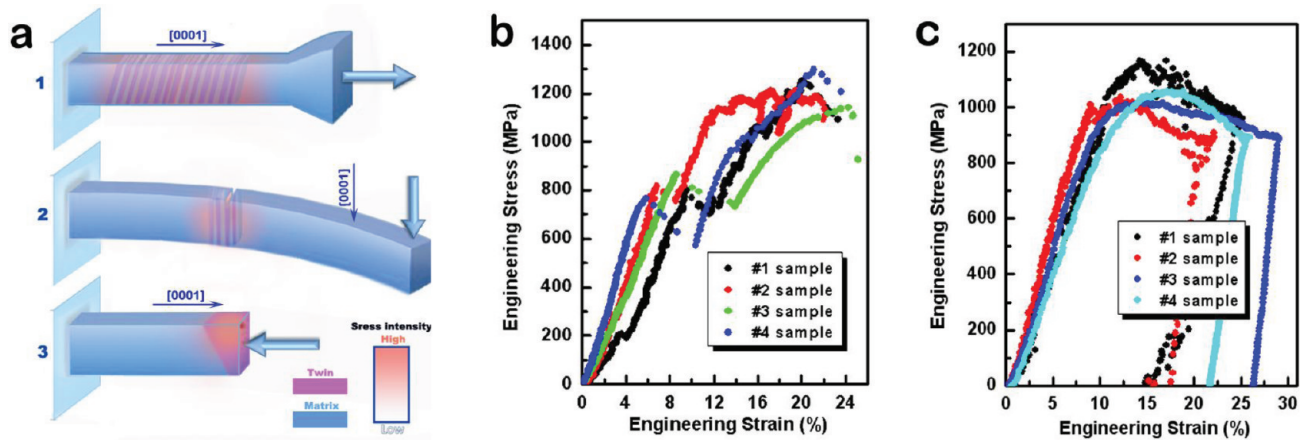


**Figure 1.** (a) A schematic to illustrate different results from 1-tension, 2-bending, and 3-compression testing. (b) Stress–strain curves from in situ tensile tests. Formation stress of twins can be read at the beginning of strain burst. Strong strain hardening was observed. (c) Stress–strain curves from in situ compression tests. Strain softening is obvious.

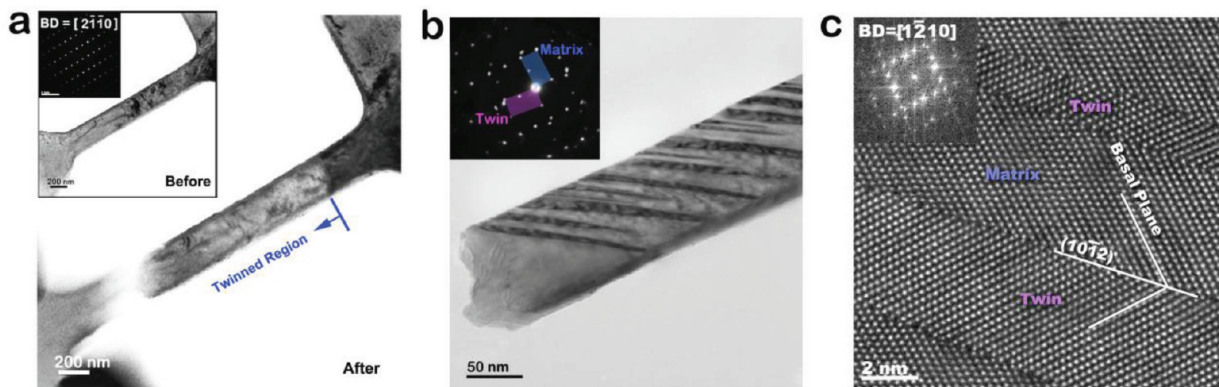


**Figure 2.** TEM images from in situ tensile tests of  $[0001]$  oriented Mg. (a) Image of tensile deformation showing the region of extension twinning. Fracture occurred at the end of the twinned region (the inset is an image of the sample before the test). The loading axis is normal to the basal plane of the crystal. (b) A bright-field image showing a nanotwin array in a tensile sample. The related diffraction pattern is inset with beam direction along  $[1\bar{2}10]$ . (c) A typical high-resolution TEM image of the nanotwinned structure from a near surface region where the finest twins were found.

Despite the critical importance of deformation twinning to Mg alloys, historically its intricate dependences on ordinary dislocation plasticity and grain size tended to confound alloy developers. Because deformation twins grow so fast, the nucleation structure is difficult to observe experimentally.<sup>3,6–9</sup> Also, it is commonly believed that deformation twinning would lose out to ordinary dislocation plasticity at smaller (submicrometer) grain sizes<sup>12,18</sup> in Mg. Unlike nanoscale twin laths in TWIP steels<sup>14,15</sup> and nanotwinned Cu,<sup>19</sup> dense arrays of coherent twin boundaries are considered difficult to introduce in pure Mg<sup>20</sup> because the twin boundary energy  $\gamma_{TB}$  is much higher ( $\sim 120$  mJ/m<sup>2</sup> in pure Mg,<sup>21</sup> compared to  $\sim 15$  mJ/m<sup>2</sup> in Cu<sup>19</sup> or hexagonal close packed Co<sup>5</sup>). As the TWIP effect scales with twin density,<sup>15</sup> the lack of nanoscale twins seems to limit the potential efficacy of TWIP for improving the mechanical properties of Mg.

Here we report in situ transmission electron microscope (TEM) observations of deformation twinning in pure Mg at unprecedented spatial resolution where the crystal size, orientation, and stress conditions at the nucleation of deformation twinning are precisely known. A nanotwinned structure is observed and its direct contribution to the mechanical properties is quantitatively studied. The quantitative compression, tension,<sup>22</sup> and bending tests were carried out in a

TEM on  $[0001]$ -oriented single crystal Mg prepared by focused ion beam (FIB) milling. Figure 1a shows a schematic of the three in situ mechanical test configurations. For details, see Supporting Information. For this orientation, basal slip is suppressed,  $\{10\bar{1}1\}$  “contraction” twinning is expected under compression,<sup>23</sup> and  $\{10\bar{1}2\}$  “extension” twinning is favored under tension. Several measured uniaxial tension and compression stress–strain curves are plotted in Figure 1b,c, where GPa-level flow stresses were achieved in our small samples, far exceeding previously measured Mg bulk strengths. On the basis of the TEM videos (see Supporting Information), the real time mechanical data and subsequent diffraction analyses, deformation twins initiated at  $\sigma \sim 800$  MPa under both tension and compression. The initiation of deformation twinning can be observed by the local change of diffraction contrast during the in situ test, since the lattice reorients in the twinned region. These deformation twinning initiation stresses are much larger than the previously reported critical resolved shear stress for  $\{10\bar{1}2\}$  and  $\{10\bar{1}1\}$  deformation twinning, which were  $\sim 3$  MPa and  $\sim 100$  MPa, respectively.<sup>13</sup> Note, however, that our stresses were measured from such small samples that they can be considered as the “local” or microscopic stresses for deformation twinning initiation, whereas the old values were bulk averaged or macroscopic stresses that do not take into

account stress amplifications needed to achieve deformation twinning. In addition, prior to twinning initiation, both the tension and compression tests demonstrated linear hardening. However, after twinning initiation, we found significant differences between the compression and tensile tests in terms of both the twin structures and the corresponding mechanical data, bringing us new insight into the mechanisms of deformation twinning.

For the compression tests, the nucleation of a single  $\{10\bar{1}1\}$  contraction twin always started from the corner of the contact surface between the sample and the indenter (see movie 1 in Supporting Information). The formation of only a single twin is presumably due to the nanolevel roughness of the contact surface, which results in stress concentrations leading to preferred nucleation sites.<sup>24</sup> This single twin grew gradually as the stress increases continuously until the twin extended across the entire width of the pillar. At this point, dislocation activity can be fully accommodated and the escape of dislocations at the surfaces results in significant strain softening, as shown in Figure 1c.

In tension, the initiation of  $\{10\bar{1}2\}$  twins results in a sudden load drop and is accompanied by a 2–5% strain burst (Figure 1b). The strain burst indicates that the total twinning nucleation volume is a large proportion of the sample volume (roughly 50%, see Supporting Information for details), which is confirmed by our TEM results. Figure 2 shows examples of the formation and structure of nanotwinned arrays formed in tension. After the nanotwins formed, homogeneous elongation was observed, mainly from the twinned region, and the tensile sample displayed a strain hardening response that led to 1300 MPa flow stress and  $\sim 20\%$  strain. Fracture occurred at the end of the twinned region (see movie 2 in Supporting Information; Figure 2a captures one of the fracture events). Compared to the ultimate tensile strength of  $\sim 120$  MPa and  $\sim 5\%$  strain in bulk pure Mg,<sup>25</sup> the mechanical properties of our small sample are impressive: on a per-volume basis our sample absorbs 2000% more mechanical energy (the average is  $\sim 1.5 \times 10^8$  J/m<sup>3</sup>) to failure than microstructure-optimized bulk pure Mg.<sup>25</sup> We regard this as approaching an upper-bound or “intrinsic” toughness of pure Mg. Another interesting point is the strain hardening process after the twin formation in tension, which is significantly different from the large strain softening we observed in compression. The near-linear strain hardening stage after the strain burst can be observed in most of the tensile curves. This response is similar to the stage 2 in plastic deformation of some bulk materials where the increase in “obstacles” produced by the activity of the primary deformation system strongly influences the activation of the secondary deformation modes.<sup>26</sup> However, in our case, strong dislocation interactions are not expected due to the small sample size and ease of dislocations escaping to the nearby surfaces. What we have instead is a large number of nanotwin boundaries that could serve as “obstacles” and harden the material. As shown in Figure 2b, in tension multiple nanotwins are distributed along the gauge section. From all the tensile samples, the most common nanotwin thickness was about 5–10 nm. High-resolution TEM analysis revealed even finer twin structures along the edge of the gage section where the spacing between twins could be only several atomic layers as shown in Figure 2c. The high density of twin boundaries restricts dislocation motion and results in strain hardening, consistent with the “TWIP” concept.

Deformation nanotwins also appeared under bending at a crack tip. One example is shown in Figure 3, where the abilities

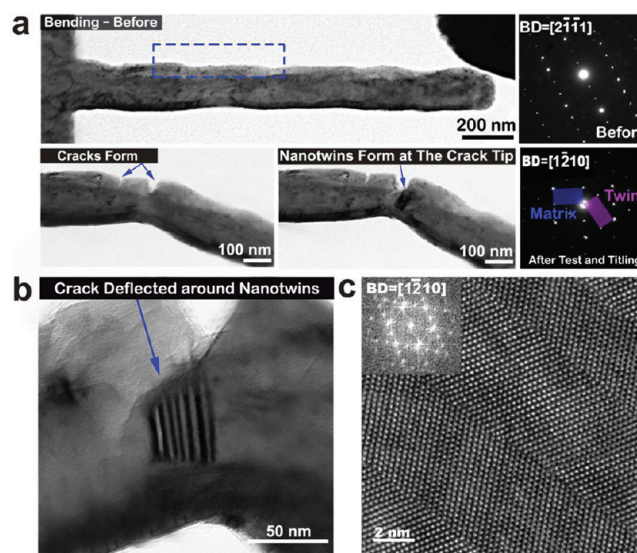


**Figure 3.** TEM images from an in situ bending test of Mg in the  $[0001]$  direction. (a) Bright-field TEM images taken from the video showing the sample before bending, at the appearance of two cracks and then at the formation of a nanotwinned region at the tip of the largest crack. Diffraction patterns from the  $[2\bar{1}11]$  zone axis show the single crystal sample before bending and the  $\{10\bar{1}1\}$  twin spots after test from  $[1\bar{2}10]$  zone axis. (b) Bright-field TEM image showing the deflection of the crack around the nanotwinned region. (c) A high-resolution TEM image showing a  $\{10\bar{1}1\}$  nanotwinned structure at a crack tip, zone axis  $[1\bar{2}10]$ .

of the nanotwins to accommodate large strain and toughen the sample are demonstrated. In the video (see Supporting Information, movie 3), two cracks can be seen to form under bending two-thirds of the way down the tensile side of the sample from the tip. In general, the crack positions varied from sample to sample, as a result of the surface roughness. In this example, as larger crack fully opened, the nanotwinned region nucleated and subsequently strongly deflected the crack as shown in Figure 3b. This is similar to transformation toughening in ceramics,<sup>27</sup> where martensitic transformations near the crack tip increase the fracture toughness, and is also consistent with previous modeling results in which a crack can stimulate twin formation.<sup>28</sup> Subsequent diffraction analysis (Figure 3a) demonstrated that the twinned region was only localized near the crack tip and was composed of  $\{10\bar{1}1\}$  contraction twins, which is not surprising given the large stress gradient.<sup>13</sup> The nanotwinned structure can be clearly seen in the HRTEM images (Figure 3c). Extension twins were also found in some bending samples, an example of which is shown in Supporting Information.

These tensile and bending experimental results give a very different picture of deformation twinning as compared to the traditional understanding where the entire lattice reorients within a twinned region. The structures are also different from so-called double twinning reported in bulk-textured Mg. In order to elucidate the origin of this high-energy nanotwinned structure, we have done a series of theoretical studies. We performed molecular dynamics (MD) simulations of single-crystal Mg tensile tests along  $(0001)$  direction (see Supporting Information for details). The results show that  $\{10\bar{1}2\}$  twins

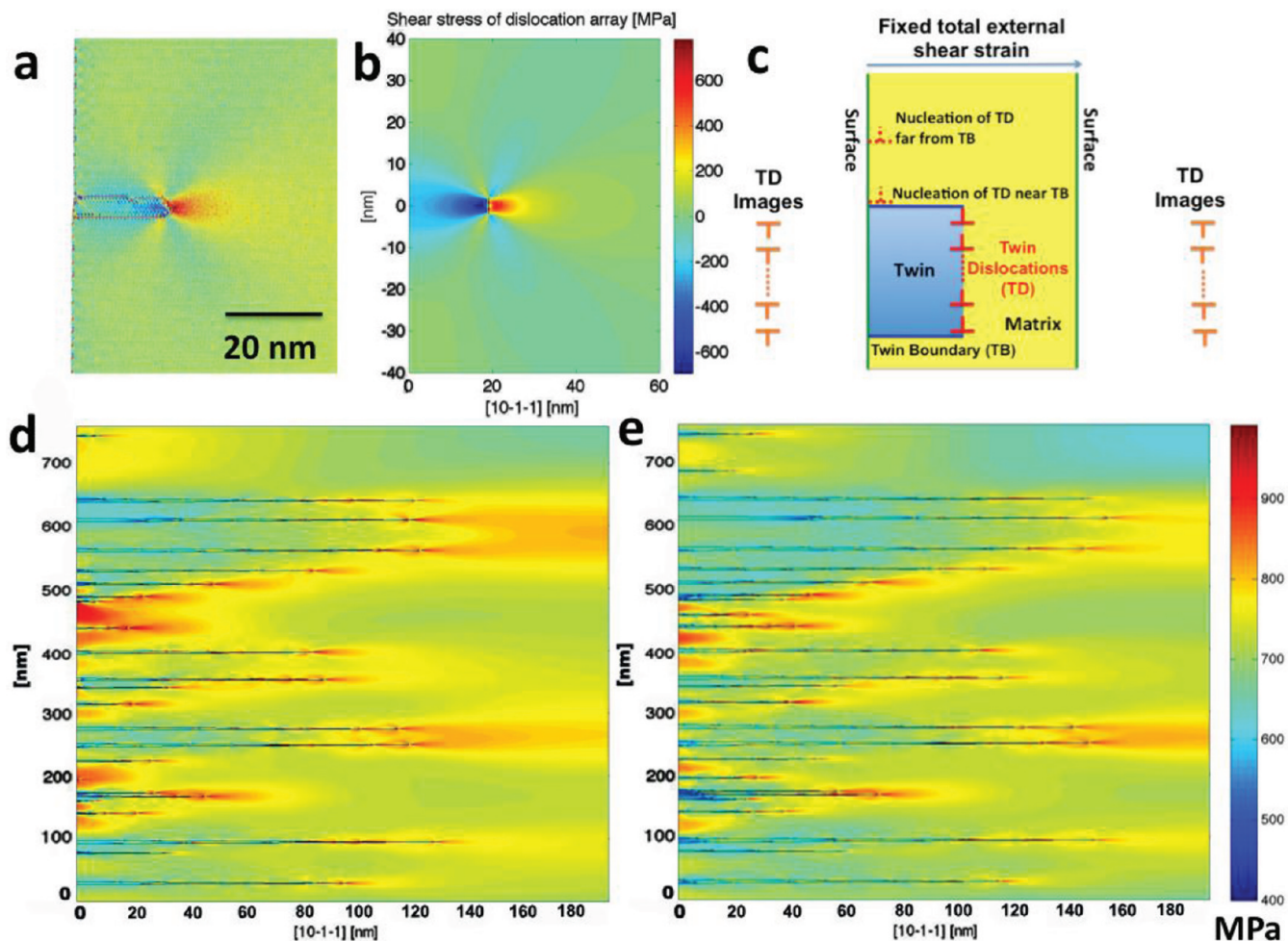


**Figure 4.** Atomic and kinetic Monte Carlo simulation results of nanotwinned structure. (a) Atomic simulation results of the shear stress field of a  $\{10\bar{1}2\}$  nanotwin in Mg nucleated from the surface. (b) Shear stress field produced by array of twinning dislocations (TD) from classical dislocation elastic theory; these TDs produce the same nanotwin as in (a). (c) Two-dimensional model of nanotwin formation by twinning dislocation nucleation and migration. The supercell is composed of parallel atomic layers as possible TD glide planes. All TDs are nucleated from the surface and only allowed to glide on one slip plane. (d,e) Kinetic Monte Carlo simulation results of nanotwins nucleating from a surface (left side) and corresponding shear stress fields based on model in (c). The twin boundaries are plotted in solid lines. Comparing the evolution from (d) to (e), we can clearly see the new TDs nucleated from high stress areas (red color) but not from the low stress areas (blue).

nucleate from surface edges and we can extrapolate that the critical nucleation stress should be about  $800 \pm 200$  MPa under low strain rates ( $10^{-2} \text{ s}^{-1}$ ), agreeing with our experiments. However, since the high strain rates ( $>10^6 \text{ s}^{-1}$ ) in direct MD simulations are not appropriate for describing the kinetics of multiple deformation twins, we need a mesoscopic model to carefully consider the kinetics of twinning nucleation and growth.

Deformation twinning is a perfectly coherent “stimulated slip” phenomenon,<sup>4</sup> which is in contrast to the less coherent “spontaneous slip” of ordinary dislocation plasticity. Slip coherency is catalyzed by promoter defects of different dimensions, which could be screw dislocations (as in the various pole mechanisms of twin nucleation<sup>3,4</sup>), surfaces or grain boundaries.<sup>29</sup> The promoter defects interact with a gliding twinning dislocation, and subsequently “infect” an atomically adjacent plane to start slipping by the same variant of the twinning dislocation Burgers vector  $\mathbf{b}_{\text{TW}}$ . Promoters of different dimensions can be dominant at different length scales.<sup>2,4,18,29</sup> In small samples or near crack tips, the dominant promoter would be the 2D free surface as shown in our MD simulations. On the

basis of this “stimulated slip” concept, we have performed mesoscale kinetic Monte Carlo (kMC) simulations to model the nanotwinning process observed in our experiments. We outline the key steps and results below, with more details in the Supporting Information.

As shown in Figure 4a,b, atomic and continuum calculations indicate that elastic incompatibilities of twinning dislocations in the sample will generate a strong elastic field that biases the nucleation rate of new twinning dislocations on a nearby surface, as

$$\nu = \nu_0 \exp\left(-\frac{Q(\sigma_s)}{k_B T}\right)$$

where  $Q(\sigma_s)$  is the stress-dependent activation energy for surface-catalyzed twinning dislocation nucleation, and  $\sigma_s$  is the shear stress at the surface.  $Q(\sigma_s)$  can be further approximated by

$$Q(\sigma_s) = Q_0 - \sigma_s \Omega$$

where  $\Omega$  is the activation volume.<sup>30,31</sup> As shown in Figure 4c, the simulation supercell is composed of parallel atomic layers as possible dislocation glide planes, and twinning dislocations can be nucleated on each layer at the surface with the same  $Q_0$  and  $\sigma_s$  initially. Once nucleated, the dislocation glides on this layer with velocity linearly dependent on  $\sigma_s$ , which is updated in the kMC model by summing the stress fields of all twinning dislocations based on classical elasticity theory. Consequently, although a twinning dislocation nucleated adjacent to an existing twin boundary has a smaller  $Q_0$  than one nucleated further from the boundary, since there would be no increase of twin boundary if an existing twin thickens, the elastic field generated by twinning dislocations of the same sign at the nanotwin tip can suppress nucleation near the twin, but promote nucleation at some distance away from the twin. As a result, the stress field of the twinning dislocations at the tip affects the nucleation of new twinning dislocations; the formation of many nanotwins is actually favored over the thickening of an individual twin (Figure 4d,e and movie 4 in Supporting Information).

The above simulation indicates high-density nanotwins can be "promoted" kinetically when high density of nucleation sites are correlated by the stress fields of twinning dislocations. Similar to surface sites in our samples, grain boundaries with high densities of dislocations can also achieve this condition,<sup>10,20</sup> thus the correlated formation of nanotwins should be a general phenomenon in deformation twinning nucleation. However, in larger crystals/grain sizes, nanotwin embryos grow to accommodate the same amount of strain, thus what is usually observed in a twinned bulk sample is the final state where multiple nanotwins have merged into a large twin, which is also predicted by our kMC model (shown in Supporting Information). In addition, inhomogeneous deformation can lead to stress concentrations and preferential nucleation sites, making it easier for a single twin to thicken, as in our compression experiments.

In summary, we have observed the fundamental embryonic structure of deformation twinning in situ in a TEM. We have directly measured the local stress to nucleate deformation twinning and the intrinsic toughness of pure Mg, both of which are much larger than presently achieved in bulk Mg, indicating large headroom for improvement. Combined with the simulation results, we believe that the formation of dense nanotwin arrays is kinetically favorable at the nucleation stage of deformation twinning even in materials with high twin boundary energies. This study develops our understanding on the kinetic nucleation mechanisms of deformation twinning and can further contribute to the future development of advanced structural materials. For example, it is conceivable that new alloys or processing schemes could be designed to take advantage of kinetics factors that would preserve nanotwinned structures to enhance strength and ductility.

## ■ ASSOCIATED CONTENT

### 📄 Supporting Information

An explanation of experimental methods as well as three in situ TEM movies for each of the three tests described and two simulation movies. This material is available free of charge via the Internet at <http://pubs.acs.org>.

## ■ AUTHOR INFORMATION

### Corresponding Author

\*E-mail: aminor@berkeley.edu.

## Author Contributions

□ These authors contributed equally to this work

## ■ ACKNOWLEDGMENTS

This research was supported by the General Motors Research and Development Center and performed at the National Center for Electron Microscopy and the Advanced Light Source at Lawrence Berkeley National Laboratory, which is supported by the U.S. Department of Energy under Contract No. DE-AC02-05CH11231. L.Q. and J.L. acknowledge support by NSF Grants CMMI-0728069 and DMR-1008104, and AFOSR Grant FA9550-08-1-0325. The authors thank U. Dahmen for thoughtful discussions.

## ■ REFERENCES

- (1) Pollock, T. M. Weight Loss with Magnesium Alloys. *Science* **2010**, *328*, 986–987.
- (2) Chen, M. W.; et al. Deformation twinning in nanocrystalline aluminum. *Science* **2003**, *300*, 1275–1277.
- (3) Christian, J. W.; Mahajan, S. Deformation Twinning. *Prog. Mater. Sci.* **1995**, *39*, 1–157.
- (4) Yu, Q.; et al. Strong crystal size effect on deformation twinning. *Nature* **2010**, *463*, 335–338.
- (5) Wang, Y. M.; et al. Achieving Large Uniform Tensile Ductility in Nanocrystalline Metals. *Phys. Rev. Lett.* **2010**, *105*, 215502.
- (6) Yoo, M. H. Slip, Twinning, and Fracture in Hexagonal Close-Packed Metals. *Metall. Trans. A* **1981**, *12*, 409–418.
- (7) Orowan, E.; Read, W. T.; Shockley, W. *Dislocations in metals*; American Institute of Mining and Metallurgical Engineers: New York, 1954.
- (8) Thompson, N.; Millard, D. J. Twin Formation in Cadmium. *Philos. Mag.* **1952**, *43*, 422–440.
- (9) Wang, J.; Hirth, J. P.; Tome, C. N. (I 0 1 2) Twinning nucleation mechanisms in hexagonal-close-packed crystals. *Acta Mater.* **2009**, *57*, 5521–5530.
- (10) Wang, J.; Beyerlein, I. J.; Tome, C. N. An atomic and probabilistic perspective on twin nucleation in Mg. *Scr. Mater.* **2010**, *63*, 741–746.
- (11) Beyerlein, I. J.; McCabe, R. J.; Tome, C. N. Effect of microstructure on the nucleation of deformation twins in polycrystalline high-purity magnesium: A multi-scale modeling study. *J. Mech. Phys. Solids* **2011**, *59*, 988–1003.
- (12) Barnett, M. R. Twinning and the ductility of magnesium alloys. Part I: "Tension" twins; Part II: "Contraction" twins. *Mater. Sci. Eng., A* **2007**, *464*, 1–16.
- (13) Koike, J. Enhanced deformation mechanisms by anisotropic plasticity in polycrystalline Mg alloys at room temperature. *Metall. Trans. A* **2005**, *36A*, 1689–1696.
- (14) Frommeyer, G.; Brux, U.; Neumann, P. Supra-ductile and high-strength manganese-TRIP/TWIP steels for high energy absorption purposes. *ISIJ Int.* **2003**, *43*, 438–446.
- (15) Bouaziz, O.; Allain, S.; Scott, C. Effect of grain and twin boundaries on the hardening mechanisms of twinning-induced plasticity steels. *Scr. Mater.* **2008**, *58*, 484–487.
- (16) Zhu, T.; Li, J.; Samanta, A.; Kim, H. G.; Suresh, S. Interfacial plasticity governs strain rate sensitivity and ductility in nanostructured metals. *Proc. Natl. Acad. Sci. U.S.A.* **2007**, *104*, 3031–3036.
- (17) Lou, X. Y.; Li, M.; Boger, R. K.; Agnew, S. R.; Wagoner, R. H. Hardening evolution of AZ31B Mg sheet. *Int. J. Plast.* **2007**, *23*, 44–86.
- (18) Barnett, M. R. A rationale for the strong dependence of mechanical twinning on grain size. *Scr. Mater.* **2008**, *59*, 696–698.
- (19) Lu, K.; Lu, L.; Suresh, S. Strengthening Materials by Engineering Coherent Internal Boundaries at the Nanoscale. *Science* **2009**, *324*, 349–352.
- (20) Wu, X. L.; et al. Deformation twinning in a nanocrystalline hcp Mg alloy. *Scr. Mater.* **2011**, *64*, 213–216.

(21) Wang, Y.; Chen, L. Q.; Liu, Z. K.; Mathaudhu, S. N. First-principles calculations of twin-boundary and stacking-fault energies in magnesium. *Scr. Mater.* **2010**, *62*, 646–649.

(22) Kiener, D.; Minor, A. M. *Nano Lett.* **2011**, *11*, 3816–3820.

(23) Miura, H.; Sakai, T. Orientation dependence of ductility of Mg single crystals at elevated temperature. *Mater. Sci. Forum* **2005**, 488–489.

(24) Kraft, O.; Gruber, P. A.; Moenig, R.; Weygand, D. In *Annual Review of Materials Research*; Ruhle, D. R., Zok, M., Clarke, F., Eds.; Annual Reviews: Palo Alto, CA, 2010; Vol 40, pp 293–317.

(25) Yamashita, A.; Horita, Z.; Langdon, T. G. Improving the mechanical properties of magnesium and a magnesium alloy through severe plastic deformation. *Mater. Sci. Eng., A* **2001**, *300*, 142–147.

(26) Kocks, U. F.; Mecking, H. Physics and phenomenology of strain hardening: the FCC case. *Prog. Mater. Sci.* **2003**, *48*, 171–273.

(27) Hannink, R. H. J.; Kelly, P. M.; Muddle, B. C. Transformation toughening in zirconia-containing ceramics. *J. Am. Ceram. Soc.* **2000**, *83*, 461–487.

(28) Fischer, F. D.; Oberaigner, E. R.; Waitz, T. Crack-stimulated twinning. *Scr. Mater.* **2009**, *61*, 959–962.

(29) Zhang, J. Y.; et al. Double-inverse grain size dependence of deformation twinning in nanocrystalline Cu. *Phys. Rev. B* **2010**, *81*, 172104.

(30) Li, J. The mechanics and physics of defect nucleation. *MRS Bull.* **2007**, *32*, 151–159.

(31) Zhu, T.; Li, J.; Samanta, A.; Leach, A.; Gall, K. Temperature and strain-rate dependence of surface dislocation nucleation. *Phys. Rev. Lett.* **2008**, *100*, 025502.